An algorithm for spike sorting with electrical artifact

Gonzalo Mena, Lauren Grosberg, Liam Paninski and EJ Chichilnisky

June 17, 2015

Abstract

We developed an algorithm that successfully automatizes spike sorting with electrical artifact. In the following, the method is succinctly described and results are shown for 56 datasets from electrical stimulation experiments

1 Introduction

In a retinal prosthetic context one is ultimately concerned with building probabilistic models of how cells responds to electrical activity. This can be thought in the same terms as in the neural coding problem, which is stated probabilistically : what is the probability of a response across a neural population given a particular natural stimulus (for example, an image)? [1]. The difference is that the stimulus is now replaced by an artificial, electrical one. Whichever model is built, data is necessary for it's fitting and for subsequently providing a solution for the inverse decoding problem: how an electrical stimulatus has to be chosen int order to elicit an arbitrary response? Naturally, the most relevant information required for the fitting of any of such models is contained in the set of stimulus-response pairs, and whereas the stimulus is controlled by the experimenter, responses (spikes) have to be identified from electrode recordings. This problem, of distinguishing particular action potentials of neurons from extracellular voltage recordings, is known in the literature as spike sorting. In consequence, any framework for achieving controlled arbitrary responses in neurons via electrical stimulation will rely on spike sorting as a fundamental building block of its computational implementation. Because of the central importance of spike sorting in systems neuroscience, in the past decades many different methodologies have been developed for automatizing the detection of spikes, and significant improvements in accuracy and computational efficiency have been achieved[2, 3, 4, 5]. However, the context of electrical stimulation constitutes a departure from the realm where current spike sorting methodologies apply, as the electrode recordings are now corrupted by the transient activity induced by this exogenous stimulation. This corruption or artifact can have an overwhelming impact in the recorded traces, making the spike identification process challenging even for of the human expert (see figure 1). Actually, previous to this work the only available spike sorting method relied heavily on human judgement, and because of the difficulty of telling spikes apart from the artifact, it was extremely time consuming even for datasets of modest size. In this article we provide the first scalable algorithmic approach for spike sorting in the presence of electrical stimulation artifact.

1.1 Electrical artifact

LAUREN HAS THINGS TO SAY ABOUT THIS, WHICH ARE THE SOURCES OF THE ARTIFACT, TRIAL BY TRIAL VARIABILITY, CHANGES IN TIME AND AMPLITUDE (INCLUDING BREAKPOINTS) DISTINCTION BETWEEN HARDWARE/AXON BUNDLE The main problem is the presence of electrical artifact, which is a consequence of the electric field generated by the stimulation, and whose ubiquitous presence hampers the spike identification process. Actually, because of the electrical artifact, whose amplitude can be several times larger than of action potentials, spikes can become almost non-identifiable: suppose for example all trials at condition j have spikes and there is little variability in spiking times. Suppose also the artifact is nearly the same across trials, so the recorded traces, assumed to be the artifact plus action potentials plus noise would look almost identical for all trials, and we may conclude that either there are no spikes at all, or that there are spikes at every trial (in which case, spiking times could be any). A more dramatic example corresponds to the situation where there is only one trial per condition. Then, spike sorting is impossible as there is no way to tell the artifact and action potential (if any) apart. The moral is that if we are completely agnostic about how artifact looks like there is little we can do. However, if we impose structure about how the artifact looks like and how often spikes should show up as a function of condition, then better chances are spikes will be identified better.

2 Methods

As shown in figure 1,trial by trial spike identification can be impossible even if templates are available. An appropriate experimental design is crucial to allow the simultaneous inference of spikes and artifact. This design should exploit neurophisiological the overcome the identifiability issues

2.1 Data description

Suppose spike sorting is required for a set of N neurons. Apart from the templates of these neurons, Data consists of a set of I voltage traces, or trials, measured both across time ($t = 1 \dots T$, corresponding to multiples of the sample rate) and a set of recording electrodes in the array ($e = 1 \dots E$), as a response to electrical stimulation (although in principle there are as many as 512 electrodes, we only consider for subsequent analysis the ones where the spike waveform have a strong enough signal, that should correspond to nearby locations of the somas of neurons) These traces are organized into a design as follows: first, a number of J different stimulus are chosen, defined by the current amplitudes of the pulses that are passed into a subset of electrodes in the array (that may or may not overlap with the recording electrodes). For separate datasets, references to specific currents and stimulating electrodes can be avoided, and replaced by the reference to the $j-th$ stimulus condition, since the stimulating electrodes remain the same and currents into each electrode always belong to the same line and increase monotonically with the index j. Then, for condition j, a number of I_j traces are available. Thus, $I = \sum_j I_j$. Naturally, templates of neurons for which spike sorting are required is done in

2.2 Assumptions

In order to come up with a generative model for which we can do tractable inferences, some assumptions have to be made. Although they are simplifications, taken together they seem to provide reasonable enough account of the data. First, we assume that spikes, artifact and noise interact linearly, and thus the observed traces are the sum of these three components (HOW CAN WE JUSTIFY THIS). Regarding the noise terms, they are assumed gaussian and trial-to-trial independent, and their variances electrode and condition dependent, reflecting different responses of the background neural tissue (which are believed to be responsible of the observed noise) to different stimulus (figure). Also, noise processes are assumed uncorrelated in in time and electrodes. This is certainly arguable: it is known that noise terms exhibit large both spatial and temporal correlations [3], but if these correlations were explicitly accounted for by the model then different covariance matrices should be estimated, one per each condition j. This would entail a non negligible additional computational burden, but most importantly, would prescribe the gathering of larger number of trials to allow reliable estimation of such matrices. As results with synthetic data created from the projection of real data on the simplified model shows that results are essentially the same regardless the correlations, and because in the first applications of this method we will deal with rather simple cases where noise correlations should not be a major issue, we prefer to maintain this assumption. Regarding the artifact, we assume it is a function of time and condition j, but remains the same for different trials. This comes from voltage recordings in TTX experiments, where no neural driven activity is expected to occur, and where it is observed that trial-to-trials variations in the traces within the same condition are well explained by the noise. The Artifact is also assumed to possess a regularized structure: both variations in time and condition (see TTX figure) are assumed smooth. Regarding activity of neurons for which we do spike sorting, we assume a set of N spike templates are available , each of them showing an action potential as recorded in all the E electrodes that are relevant for the analysis. Rather than an assumption, this is a reality as templates are available from previous experiments using visual stimuli, where no electrical artifact is expected. The actual underlying assumption is that templates faithfully describe the real action potentials, as they are are subject to all the estimation problems related to regular spike sorting(IS THIS THE RIGHT PALCE TO TALK ABOUT HOW TEMPLATES ARE OBTAINED?). For spike timing, it is assumed that spikes can occur only over a set of T' consecutive multiples of the sample rate, denoted $\{t_1, \dots t_{T'}\} \subseteq \{1 \dots T\}$. Again, this is to keep a tractable setup, since a model that allows spiking at arbitrary times, as the one developed in [6] would require computations that for now can be avoided. Also, we assume at most one spike per neuron can occur in the recording time, which is a consequence that spikes are sought in a time window that is no bigger than the usual refractory period (cite). Finally, for spiking probabilities, an underlying parametric model for the activation curves is assumed, reflecting the known sigmoideal response saturation phenomenon, which is also observed in the electrical stimulation context. (CITE about activation curves). The need of making this assumption will be clear after the generative model and algorithm for it's fitting are introduced, which is done in the following.

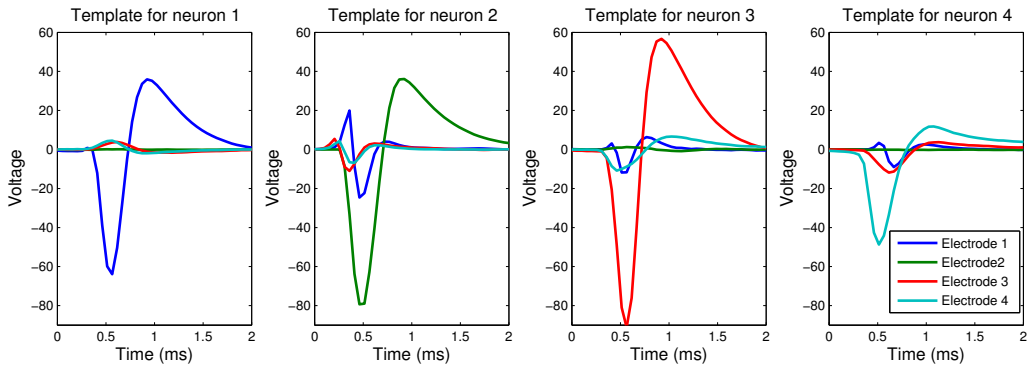

Figure 1: Examples of action potential templates (four neurons), as recorded in four electrodes.

2.3 The generative model

Now we provide the mathematical details about the data generating process. The ultimate goal will be to make inferences about the variables that represent the artifact and spikes. Denote $Y_{t,e}^{i,j}$ the observed voltage for trial i of condition j at time t and electrode e. Then the model is

$$Y_{t,e}^{i,j} = A_{t,e}^{j} + \sum_{n}^{N} (K_n s_n^{i,j})_{t,e} + \epsilon_{t,e}^{i,j} \quad \epsilon_{t,e}^{i,j} \sim \mathcal{N}\left(0, \sigma_{e,j}^2\right) \quad \text{i.i.d} \tag{1}$$

Here $A_{t,e}^{j}$ is the artifact at time t, electrode j and condition j, and $s_n^{i,j}$ is abinary vector containing spiking information for neuron n at trial i of condition j: $s_n^{i,j}(l) = 1$ if spike occurs at time t_l. Since at most one spike per neuron occurs for a single trial, $\sum_{l=1}^{T'} s_n^{i,j}(l) \leq 1$. K_n is a $(T \times E, T')$ convolution matrix whose rows contain copies of action potentials for neuron n as recorded in all electrodes, but with spike onset aligned at all different possible spike times. For notational convenience, we also consider a vectorized version of equation (1), in which voltage traces are concatenated across time, electrode, trial and condition, to generate a unique huge vector Y. The same can be done with the artifact, spikes and neurons. This leads to the re-statement of equation (1) as

$$Y = XA + Ks + \epsilon \tag{2}$$

Where $\epsilon \sim \mathcal{N}(0, \Sigma)$, Σ with diagonal given by the $\sigma_{e,j}^2$'s and X is the covariate matrix that indicates which artifact variables are active in the different positions of the vector Y. Equivalent, in terms of the likelihood

$$p(Y|A, s, \Sigma) \propto \exp\left(-\frac{1}{2}(Y - XA - Ks)^t \Sigma^{-1} (Y - XA - Ks)\right)$$

In the following, we use both the vectorized and not vectorized notations interchangeably. Notice until now nothing has been said about the explicit structure of the artifact in the model, which needs to be constrained to avoid overfitting. We impose regularity constrains that aim to reflect our knowledge of the artifact shape, as discussed in (WHERE?). Hardware breakpoints induce, in each recording electrode, a partition of the set $\{1 \dots J\}$ into $B(e)$ inter-breakpoint ranges, denoted $\{b(j', e)\}_{j'=1 \dots B(e)}$. With this notation, regularity constraints are of the form:

$$\sum_t \sum_j ||A^j_{t+1,e} - A^j_{t,e}||^2, \;\; \forall e = 1 \dots E$$

$$\sum_{j \in b(j',e)} \sum_t ||A^{j+1}_{t,e} - A^j_{t,e}||^2 \,; \; e = 1 \dots E, \forall j' = 1 \dots B(e)$$

They are essentially smoothness constraints, both in time and conditions within the same inter-breakpoint range. These can ultimately be represented as products $A^t D_k A$ for suitable semi positive definite matrices D_k. Also, for numerical stability we also consider an overall regularization (it's corresponding D_k is equal to the identity). We use squared l_2 regularization instead of l_1 regularization, (as in the fused lasso CITE) because we will exploit heavily the gaussian conjugacy that is entailed by the l_2 framework, and because we are not making any assumption about sparsity of artifact variables. The amount of regularization in each of these terms is controlled by some regularization hyperparameters, denoted λ_k. Thus, our knowledge about artifact smoothness is expressed as the following gaussian prior

$$p(A|\lambda) \propto \exp\left(-\frac{1}{2}\sum_k \lambda_k A^t D_k A\right)$$

For the spike probabilities, we assume a logistic regression prior for each neuron. That is, the variables $r^{i,j}_n = \sum_l s^{i,j}_n(l)$ are conditionally independent given the logistic regression parameters $\alpha_n = (\alpha^1_n + \alpha^2_n)$ $p(r^{i,j}_n = 1|\alpha_n) = \dfrac{1}{1 + \exp\left(-\alpha^0_n - j\alpha^1_n\right)}$. Regarding spike times, we don't make any explicit assumption (DISCUSS IN FURTHER DIRECTION): we set a uniform prior on the times t_l.
Finally, for the entries of the diagonal of the matrix Σ,, the variances $\sigma^2_{e,j}$ we consider a non-informative prior for the joint:

$$p(\sigma^2_{e,j}, e = 1 \dots E, j = 1 \dots J) \propto \prod_{e,j} \frac{1}{\sigma^2_{e,j}}$$

Again, this choice is made to exploit conjugacies.

2.4 Relation to other methods

FILL WITH REFERENCES AND DISCUSSION ON WHAT WE ARE TAKING FROM OTHERS, AND WHAT NO

3 The Algorithm

The algorithm we introduce here is concerned with the inference of the variables for the posterior distribution spawned by the data likelihood and the priors corresponding to the constrains in the parameters. It is important to mention that although all priors are log concave, the log posterior is not concave, because of the variables $s^{i,j}_n$, which are defined in a non concave space. If these variables were fixed to arbitrary values, then the log posterior would become

concave, therefore, the number of local optima could grow exponentially with the number of trials and neurons. Many of these local optima will have a small probability, and thus if we constrain the search to the region of the parameter space where the posterior is high, better chances are that meaningful results will be obtained. We handle that problem by taking initial values provided by a convex relaxation (SEE BELOW?) of the original problem. Notice, however, there is no reason to believe that the maximum of the posterior will provide the right spike sorting solution: we make strong assumptions about the data generating process, which can be reasonable as a first approximation, but there are other phenomena that are not being accounted for by the model (for example, spiking of neurons for which templates are not available), and thus there is not a sharp correspondence between what is told by the model and what happens in reality. For this reason we don't seek for the MAP solution (CITE); instead, we perform bayesian inference, implemented as a Gibbs sampler that exploit the inherent conjugacies of the model. In this sampling setting the question is how to transform the obtained samples in a spike sorting solution. It is the case that the Gibbs sampler rapidly lead to convergence of the variables s (FIGURE MAYBE?) that barely change after some iterations, while the rest have only small fluctuations. Roughly speaking, the Gibbs sampler gets stuck at a local solution for s. The question that arises is again, even if this solution should be more robust that the one obtained via optimization (coordinate ascent), how can we tell if it is a meaningful one or not. We address this question by looking at a certain aspect of the residuals, so if a huge mismatch is detected between the current fit to the model and data, changes are made to the current solution to allow a 'jump' from the current local solution to an eventually better one. This procedure is of heuristic nature: misspecification plus lack of log concavity render the problem a difficult one, From the likelihood plus the constrains imposed on the parameters we obtain a bayesian model, and our algorithm will be concerned with the inference of the variables the first impulse is to follow the MAP approach: what are the most likely spike allocations and artifact that allow us to explain the data, given our prior knowledge? There are, though, several caveats: First, the introduction of the binary vector s renders the problem non convex, which implies many local optima may exist. Thus, we are at risk of obtaining meaningless local solutions. Also, there are regularization hyperparameters that need to be estimated somehow. Third, all models are wrong and, as a consequence, there is not guarantee that MAP solution will provide the right spike sorting. To address these issues, and improve robustness to model misspecification and initial values, the inference procedure is divided into four stages steps, which, put together, give rise to the spike sorting algorithm

3.1 Initialization

As mentioned before, multimodality implies that any optimization (or sampling) procedure is prone to fall into local optima, and this local optima may be non interesting. It is of critical importance to come up with good initial estimates of the parameters in order to avoid such situations. To this end, we consider initial values provided by a convex relaxation, explained below.

3.1.1 Convex relaxation via SOCP

We turn the original estimation problem into a convex one by allowing the binary vectors $s_n^{i,j}$ belong to the $T'-$simplex: $0 \leq r_n^{i,j} \equiv \sum_{l=1}^{T'} s_n^{i,j}(l) \leq 1, 0 \leq s_n^{i,j}(l) \leq 1$. In this new

setting we no longer look for spikes but rather 'generalized spikes', and the presence or absence of spikes at certain times is replaced by spike probabilities. Unfortunately, even if the new problem is already convex, there are some nonlinear dependencies (for example, with the logistic regression, artifact regularization and variance priors) that impose hard computational constraints for the maximization of the log posterior. Thus, our approach is to re-state an approximation of our already convexified problem in a framework for which a number of efficient solvers are available. To this end we profit from the Second Order Cone Programing (SOCP) theory, in which a linear function is minimized, subjected to conic constraints. The question is how to come up with an approximation that captures the spirit of the original program. We take the following approach: to avoid artifact regularization hyperparameters, we consider instead a simple polynomial model; artifact is unconstrained in time but assumed a polynomial function of condition (with conditions in the same set $b(j')$). This leads to the replacement of artifact XA by a product $X'A'$, with A' the new artifact variables and X' representing covariates in this polynomial representation. The logistic regression prior is replaced by the (linear) constraint that spiking probabilities increase with condition, for each neuron. That is, for $j = 1 \dots J-1$ and $n = 1 \dots N$ we set $\sum_{i,l} s_n^{i,j}(l) \leq \sum_{i,l} s_n^{i,j+1}(l)$. Finally, the non-informative prior for the variances is just avoided.

Before stating the SOCP in detail, notice that artifact and spike variables can be concatenated, by defining $z = (A', s)$. In the same vein, the artifact plus (generalized) action potential term can be expressed as a unique matrix product between some matrix M and z.

Now, let's construct the new program: first, to make the relaxation as similar to the original program as similar as possible, we will look for sparseness in the generalized spiking vectors. This translates in imposing not only simplex constraints but also in penalizing spiking in the objective function via the linear term $\sum_{j,i,n,l} s_n^{i,j}(l)$. Notice this will naturally induce sparseness, as $s_n^{i,j}(l) = |s_n^{i,j}(l)|_1$. With this, we now need to state we want to explain our data (log likelihood). We do so by a quadratic term for each condition: we want the RSS $||Y - Mz||^2$ to be as small as possible. To meet the linear objective requirement for a SOCP, we use duality and introduce the auxiliary variable ρ in the objective and constraint $||Y - Mz||^2 \leq \rho$. The trade-off between explaining of the data and sparseness is modulated by the hyper parameter κ, which is set beforehand.

Summarizing, we aim to solve the following problem

$$\min_{z=(A',s),\rho} \quad \sum_{j,i,n,l} s_n^{i,j}(l) + \kappa\rho \tag{3}$$

$$\begin{aligned}
\text{s.t.} \quad & 0 \leq \textstyle\sum_{l=1}^{T'} s_n^{i,j}(l) \leq 1 \;\; \forall i,j,n \quad 0 \leq s_n^{i,j}(l) \leq 1 \;\; \forall i,j,n,l \quad \text{generalized spikes} \\
& \textstyle\sum_{i,l} s_n^{i,j}(l) \leq \sum_{i,l} s_n^{i,j+1}(l) \quad \forall n, j = 1 \dots J-1 \quad \text{increasing spiking probabilities} \\
& ||Y - Mz||^2 \leq \rho \qquad \text{Explaining data}
\end{aligned}$$

There are two concerns with this formulation: first, different choices of the new parameters (κ, and the degree of the polynomial) will lead to different initial solutions. However, results show that it is a good choice to set high values of κ, which represents the importance of explaining the data over sparseness of the generalized spikes. For the degree of the polynomial, satisfactory results are achieved with a quadratic model. There is no need to increase this degree further as this would lead to more variables, and as a result, slower computations.

Also, as mentioned above, we are solving an approximation, and for example, the obtained spike probability v.s. condition curves (thereon spike activation curves) may look non-smooth. However, again results show the approximated results provided by this SOCP are good enough to provide initial estimates for the variables of the problem. Now we give details about how to obtain initial values of the variables given the solution of the SOCP.

3.1.2 Initialilzation of A, Σ, α and λ

Obviously, initial value for the artifact will be given by $A_0 = XA'$, where A' is the solution of the SOCP. Also, for Σ_0 we look for the residuals at different conditions and electrodes, leading to $\sigma^2_{j,e_0} = \frac{1}{TI}||Y_{j,e} - M_{j,e}z||^2$ where $Y_{j,e}$ and denotes the sub-vector of Y obtained by considering only samples in condition j and electrode e, and $M_{j,e}$ is the sub matrix of M constructed in a similar manner. [1]

For α, the parameters of the logistic regressions, we consider a least square fit with the activation curves. Finally, for λ, we carry out maximization of $p(A_0|\lambda)$ with respect to λ. This leads to the following problem

$$\lambda_0 = \arg\min_\lambda \tfrac{1}{2} A_0^t \left(\textstyle\sum_k \lambda_k D_k\right) A_0 - \log \left| \textstyle\sum_k \lambda_k D_k \right|$$
$$\text{s.t.} \quad \lambda \geq 0$$
$$\textstyle\sum_k \lambda_k D_k \succ 0$$

The above (convex) problem is known in the literature as *maxdet*, and to solve it we use gradient descent. Notice the only parameter we have not initialized is the first estimate of the spikes s_0. However, this is not necessary, as this will arise as a consequence of the next step of the algorithm: Gibbs sampling. For now, it is enough to have initial estimates of the generalized spikes, which were given by the SOCP.

3.2 Gibbs sampling

Given our initial solution we would like to converge to obtain good local optima of the posterior. That can be done via coordinate descent between A, s, Σ, α and λ. However, to keep the probabilistic set up in mind, and to allow more variability in solutions (and a better exploration of the parameter space) we prefer a block Gibbs sampling approach. Notice that in any case solutions shouldn't be very different (and they are not in practice), as the posterior is highly peaked in the modes, given the overwhelming weight of the likelihood. Thus, coordinate descent becomes essentially equivalent to Gibbs sampling, where the samples will correspond (approximately) to the modes.

Now we detail the several stages of the Gibbs sampler

[1] Notice the above estimates are biased and should be corrected by the number of degrees of freedom, however, this has little impact in results and thus this further step is avoided.

3.2.1 Sampling from spikes

The conditional spike probabilities for a neuron at a given trial and condition, given all the rest of the variables and data is multinomial:

$$p(s_n^{i,j}(l) = 1|Y, A, \Sigma, \lambda, \alpha, s\backslash_n^{i,j}) \propto \frac{p(r_n^{i,j}(l) = 1|\alpha_n)}{T'} \exp\left(-\frac{1}{2}\sum_e \frac{||Y_e^{i,j} - \sum_n (K_n s_n^{i,j})_e - A_e^j||^2}{\sigma_{e,j}^2}\right)$$

Notice posterior spike probabilities of a given trial don't depend on other trials or conditions. However, spiking in one neuron does depend on spiking from others. This leads to a sequential sampler: we iteratively sample from different neurons while keeping spikes of the others fixed, and within each neuron, we sample all trials and conditions.

3.2.2 Sampling from the artifact

Denoting $\Lambda = (\sum_k \lambda_k D_k)^{-1}$ we have the following expression for the conditional distribution of the artifact, conditional on the rest of the variables and data.

$$A|Y, s, \Lambda, \Sigma, s, \alpha \sim \mathcal{N}(\mu, \Sigma') \quad \Sigma' = \left(X^t\Sigma^{-1}X + \Lambda^{-1}\right)^{-1} \quad \mu = \Sigma' X^t \Sigma^{-1}(Y - Ks),$$

3.2.3 Sampling from Σ

Sampling is straightforward once noticing that the conditional distribution of $\sigma_{e,j}^2$ conditional on data and the rest of variables is inverse gamma:

$$\sigma_{e,j}^2|Y, s, A, \alpha, \lambda, \sigma^2\backslash_{e,j} \sim \text{ Inv-Gamma}\left(\frac{ITE - 1}{2}, \frac{1}{2}||(Y - AX - Ks)_e^j||^2\right)$$

3.2.4 MAP for α

Notice we implicitly assume a flat prior for α. One may sample from it's posterior distribution, but in order to keep simplicity we prefer a maximization approach [2]:

$$\max_\alpha p(\alpha|s, A, Y, \Sigma, \lambda) \propto \prod_{i,j,n} \frac{1}{1 + exp\left(-(2r_n^{i,j} - 1)(\alpha_n^0 + j\alpha_n^1)\right)}$$

The above maximization corresponds is achieved by performing N separate logistic regressions, one per each neuron.

Regarding λ, we don't further modify from this variable from its inicial value. There are two reasons for not doing so: first, we may end up in artifact overfitting, so it is preferable to have a value of this hyper parameter as a 'point of truth'. We have already obtained an estimate for this value, λ_0, and results show this choice is already good enough. Also, optimizing λ via solving the maxdet problem at each iteration would create a huge computational bottleneck.

Via repeated iterations of the several stages of the Gibbs sampler, convergence to points close to local optima is achieved. Hopefully this solution corresponds to the right spike sorting, and this is the case sometimes, but in general one may obtain nonsensical spike trains: the most

[2] Notice by doing thus we no longer have a *bona fide* Gibbs sampler, but instead, a Gibbs-EM hybrid

typical situations corresponds where the spike sorting is correct for some conditions, but there are others in which no spikes are found, where in reality all trials have spikes, or vice versa. Also, it is possible to infer spike in all trials while spikes are present only in some of them. Fortunately, there are ways to diagnose this pathological, though common, situations, and these diagnostics allow us to come up with the last part of the algorithm, which is a post-processing heuristic that introduces local changes in the Gibbs sampling solution, in order to improve the fit in the aspects where an overt lack of sense has been diagnosed.

3.3 Post processing

There are two ways to assess the plausibility of solutions provided by Gibbs sampling: the first of them is to look at the RSS at each condition. In conditions where the fit is poor these residuals should be higher. The problem of just looking at the residuals is that there are other reasons that could make the RSS to be high: the response of the neural system changes from one condition to the next, and there are phenomena characteristic to each condition but not accounted for by the model that explain significant conditions

A more amenable alternative comes from assessing differences between empirical spiking probabilities at each condition, $\sum_i r_n^{i,j}/I$, and probabilities of spiking provided by the logistic regression, $\hat{p}(r_n^{i,j} = 1)$. As we are confident that logistic regression is a good description os reality, lack of fit in this aspect of the model diagnoses the attained solution doesn't explain data in the desired sense. In those cases, something is needed to be done to 'jump' from this local optima into a better one. This is done by re-sampling the artifact in the conditions where the fit is worst conditional on the rest of the sampling from the conditional (prior) distribution of the artifact given the rest of the conditions. That is, if J_1 is the set of such conditions, we re-sample the artifact from $p(A_{J_1}|\lambda, A\backslash_{J_1})$. Sampling is straightforward because of the gaussianity of the above conditional distribution. In other words, we 'borrow' statistical strength from places where we are confident the fit is good. The above idea can be implemented as an heuristic: briefly, re-sample the artifact and with this new estimate re-sample spikes and the rest of variables. Assess the fit again, until we cannot reject the hypothesis that spikes come from a logistic regression model (using a chi squared test, see [7]) , or until a maximum number of iterations is exceeded. Notice this is similar to the use of the minimum discrepancy $D_{\min}$ [8] in a posterior checking framework, but unfortunately we were not able to explore other bayesian criticism measures [9], because of the difficulty of sampling from this highly peaked and multimodal posterior distribution.

Before comenting results, in figure 2 are shown all the stages of the algorithm in a sample dataset.

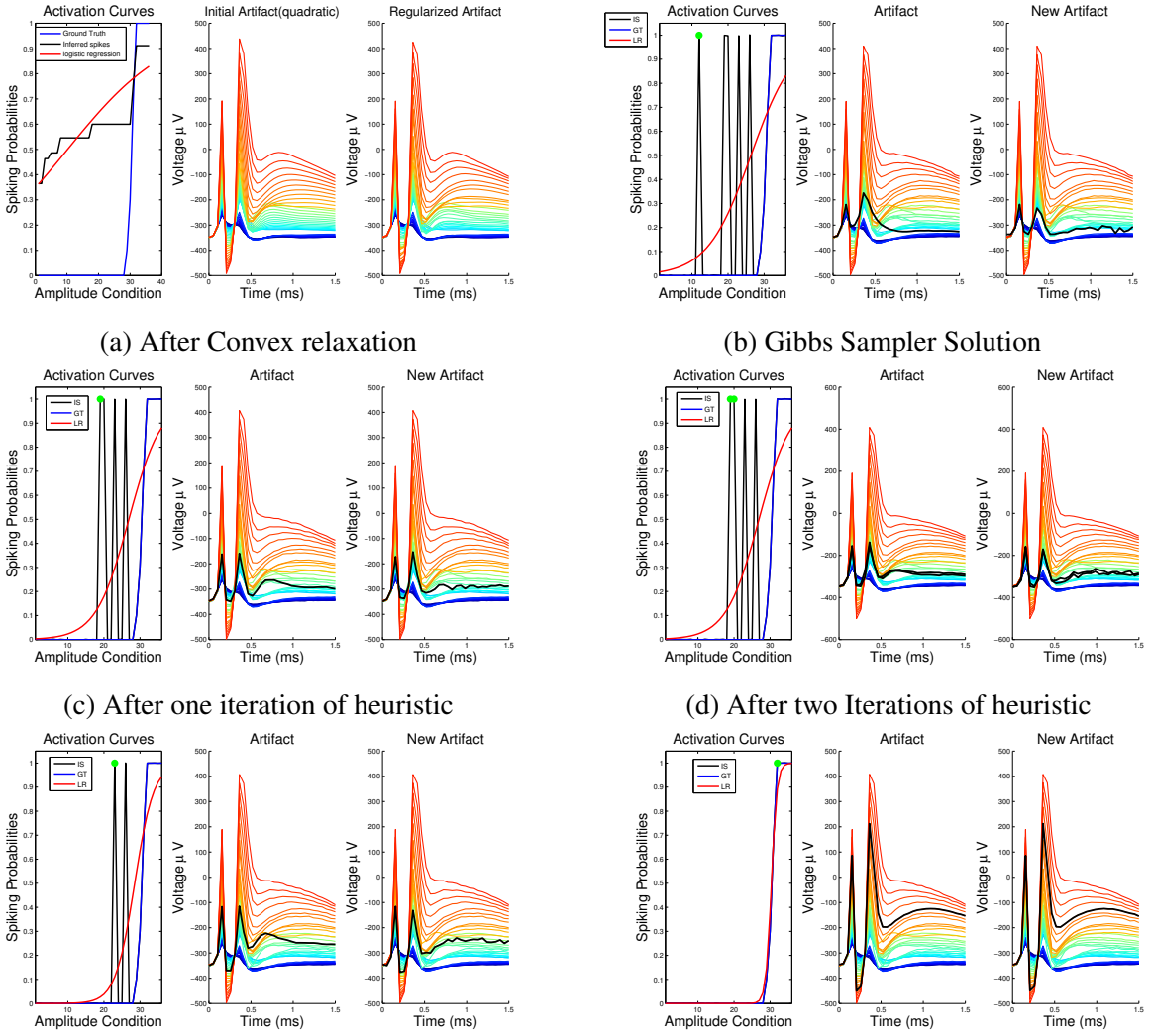

(a) After Convex relaxation

(b) Gibbs Sampler Solution

(c) After one iteration of heuristic

(d) After two Iterations of heuristic

(e) After three Iterations of heuristic

(f) Final Result

Figure 2: Illustration of the different stages of the algorithm. Initial values provided by the convex relaxation (a) are used as input for the Gibbs sampler (b). If the fit of the activation curve to a logistic model is poor, the artifact is resampled in the conditions that are most responsible of that lack of fit (c,d,e), until no changes are further needed (f)

4 Results

The algorithm was tested in 56 datasets in which spike sorting was required for 4 neurons (templates in the electrodes used are shown in figure 1). For all of them the number of amplitude conditions was 17, and for each condition there were either 20 or 10 trials. In the former performance was almost perfect, with an overall error rate of 0.71% (see table 1 for summary results for each neuron and figure 3 for the true and estimated activation curves). However,

in the latter the error rate was higher, reaching 10.9% (see table 2 for details), possibly due to the limitations posited by the fewer number of trials. As we aim to decrease the error rate to zero, it is important to understand better which are the causes of failures: Better models can be built if these causes are well understood, and even with the current model this understanding could be used to inform the human expert when the causes are present. It turns out that the unwanted activation of an axonal bundle is the phenomenon that explains the best failures in spike sorting. In the following we show how this axonal activation hampers spike sorting, and how to deal with it in the absence of a better model

	Trials w. spikes	Failures in detection	Trials w. no spikes	False positives	Total
Neuron 1	1040	43 (4.1 %)	2190	73 (3.3%)	3230
Neuron 2	329	0	2901	1 (0.03%)	3230
Neuron 3	546	0	2684	0	3230
Neuron 4	310	0 (.64%)	2920	39 (1.33%)	3230

Table 1: Overall results for all the analyzed neurons (only 10 datasets with 20 trials per condition)

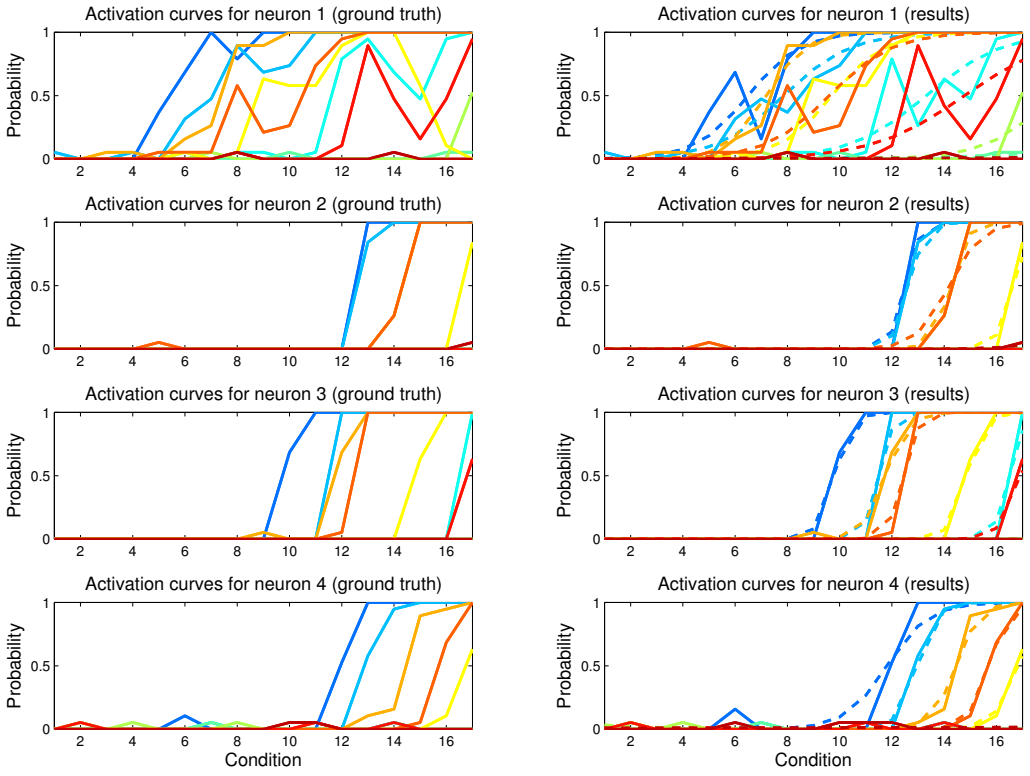

Figure 3: Activation curves, ground truth (left) and model results (right). Each trace corresponds to a dataset. In the plots to the right are also shown (dashed lines) the logistic regression fits

	Trials w. spikes	Failures in detection	Trials w. no spikes	False positives	Total
Neuron 1	4328	1019 (23.5%)	5940	490 (8.26%)	10268
Neuron 2	3515	689 (19.56%)	6236	519 (7.68%)	10268
Neuron 3	1498	0	8488	282 (3.22%)	10268
Neuron 4	2143	124 (5.79%)	7159	491 (11.89%)	10268

Table 2: Overall results for all the analyzed neurons (all the 56 datasets)

4.1 Misspecification due to axonal activation

It has been recently documented [10] that besides action potentials elicited by the targeted electrical stimulation of somas, there can be unwanted activation of axons. This activity can also be detected in electrode recordings, and although it is still not completely understood, it is known that begins to appear at a similar amplitude that of somatic spikes. However, unlike somatic spikes, the magnitude of this aggregated activation of axons increases with stimulus amplitude, and the activation curves of these axonal activities tend to be much sharper than of spikes. Because of this, templates are not available for this bundle activation and as a result it cannot be easily accounted for in the current framework.

Axonal activation thus leads to model misspecification, and the question is to which extent our misspecified model can still be useful to detect spikes, in other words, will this phenomenon affect algorithm performance, and if it does, is it possible to inform a possible failure, in order to proceed with manual detection?

To address this questions we proceed via examples. In figure 4 is shown an example of successful detection (although it doesn't coincide with ground truth) regardless of the presence of axonal activation. This example serves to illustrate a way in which axonal activation interacts with the rest of the components of the model: here, spikes have a bigger magnitude than the corresponding template, and this is explained by the overlap in time of somatic and axonal spikes. Thus, we detect onset of axonal activation by increased residual variance σ (in this case conditions 11 or 12). Also, once axonal activation becomes less variable in time, it is treated by the algorithm as being part of the artifact, which explains the difference in red and black traces at conditions 14 and 15. There are some cases, however, where the spike shapes change so much due to axonal activation that the templates are not good enough to explain the residuals and as a result spikes are failed to be detected. This is a rare situation, and again, it should be identified by an increased residual variance. An example of failure is shown in figure 5. There are conditions (e.g. 6,7) in which clusters naturally into three classes: no spiking, spiking and spiking plus axonal activation. At conditions 7 and 8 spikes are not detected, and only spike plus axonal activation trials are considered as true spikes (in fact, the same judgement was made by the human at condition 8). To understand how things can go wrong here it is important to look at the residuals: In some sense, it is also a meaningful interpretation to believe blue traces in condition 7 have no spikes, because if that was the case the spike template would fairly match the residuals. This example shows how spike sorting requires a level of expertise that is beyond what can be stated in the model. However, again in this case presence of axonal activation is indicated by increased residual variance, which can be informative for the experimenter. Other examples (not shown here) include similar situations, and an erroneous spike detection could be detected by a lack of fit between the activation curves and the underlying

logistic model. Finally, another measure that can be informative comes from the regularization prior: basically, one can ask the question of how plausible is our artifact estimate given our prior artifact specification. If not, that could indicate that a artificial breakpoint should be added to the model in order to properly account for the changes in the artifact induced by the axonal activation.
Summarizing, this modeling framework is not exempt of risks due to misspecification, but we can evaluate the goodness of fits by looking at different relevant aspects of the model: underlying spike probabilities, residual variances, and prior artifact specification. Taken together they should lead to relevant information about possible lack of fit, causes of this lack of fit (axonal activation) and ways in which this lack of fit could be driving the results wrong.

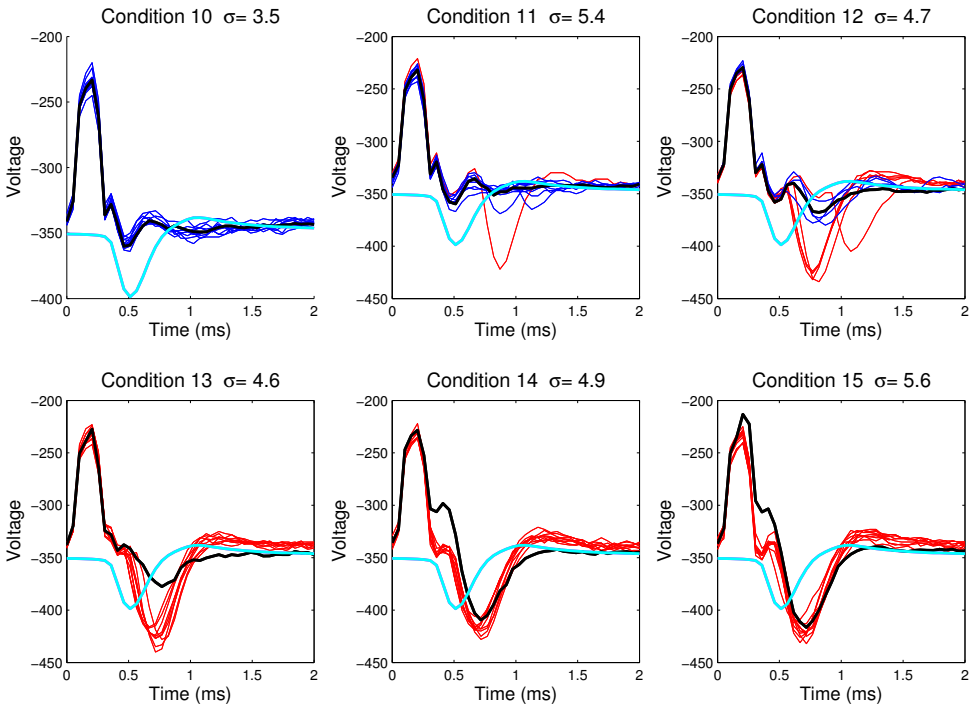

Figure 4: An example of successful detection with axonal activation. Cyan trace: spike template, blue traces: trials with no spike, red traces: trials with spikes, black: artifact estimate

References

[1] Liam Paninski. Maximum likelihood estimation of cascade point-process neural encoding models. *Network: Computation in Neural Systems*, 15(4):243–262, November 2004.

[2] M. S. Lewicki. A review of methods for spike sorting: the detection and classification of neural action potentials. *Network: Computation in Neural Systems*, 9(4):53–78, 1998.

[3] Jonathan W. Pillow, Jonathon Shlens, E. J. Chichilnisky, and Eero P. Simoncelli. A model-based spike sorting algorithm for removing correlation artifacts in multi-neuron recordings. *PLoS ONE*, 8(5):e62123, 05 2013.

[4] Chaitanya Ekanadham, Daniel Tranchina, and Eero P. Simoncelli. A unified framework and method for automatic neural spike identification. *Journal of Neuroscience Methods*, 222(0):47 – 55, 2014.

[5] Hernan Gonzalo Rey, Carlos Pedreira, and Rodrigo Quian Quiroga. Past, present and future of spike sorting techniques. *Brain Research Bulletin*, 2015. In press.

[6] Chaitanya Ekanadham, Daniel Tranchina, and Eero P. Simoncelli. A blind sparse deconvolution method for neural spike identification. In John Shawe-Taylor, Richard S. Zemel, Peter L. Bartlett, Fernando C. N. Pereira, and Kilian Q. Weinberger, editors, *NIPS*, pages 1440–1448, 2011.

[7] Hosmer W., Hosmer T., Le Cessei S., and Lemeshow S. A comparison of goodness-of-fit tests for the logistic regression model. *Stat Med*, 16(9):965–980, 1997.

[8] Andrew Gelman, Xiao li Meng, and Hal Stern. Posterior predictive assessment of model fitness via realized discrepancies. *Statistica Sinica*, pages 733–807, 1996.

[9] George E.P. Box. Sampling and bayes' inference in scientific modeling and robustness. *Journal of the Royal Statistical Society, Series A*, 143:383–430, 1980.

[10] Lauren E. Grosberg, Pawe Hottowy, Lauren H. Jepson, Shinya Ito abd Frederick Kellison-Linn, Alexander Sher, and Wadysaw Dabrowski abd Alan M. Litke abd E.J. Chichilnisky. Axon activation with epiretinal stimulation in isolated primate retina. In *The eye and the chip*, 2014. Conference Poster.

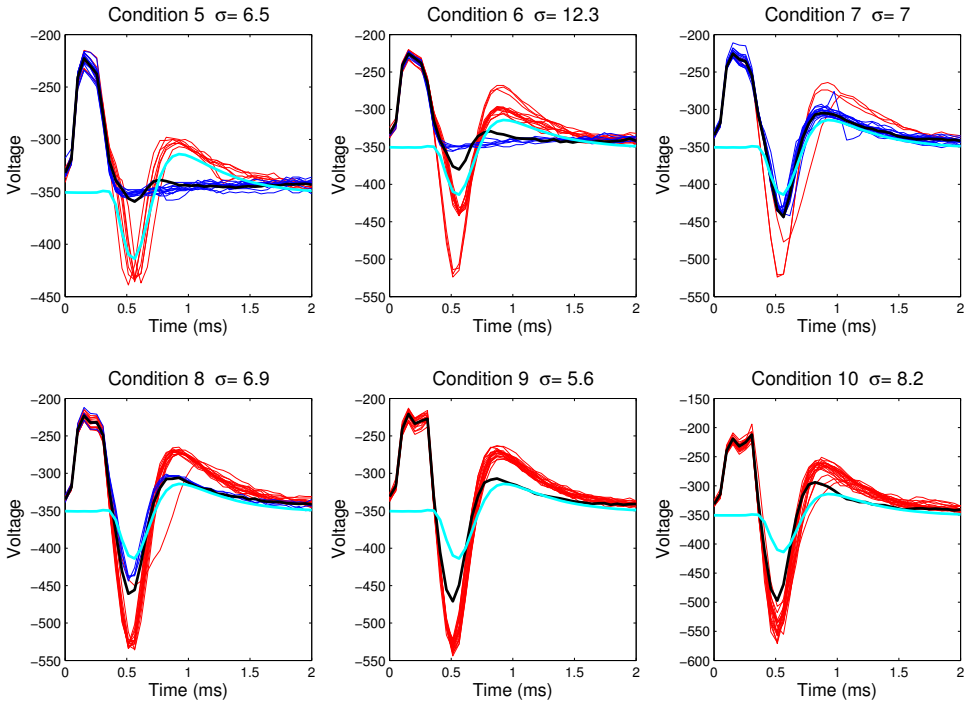

(a) Traces

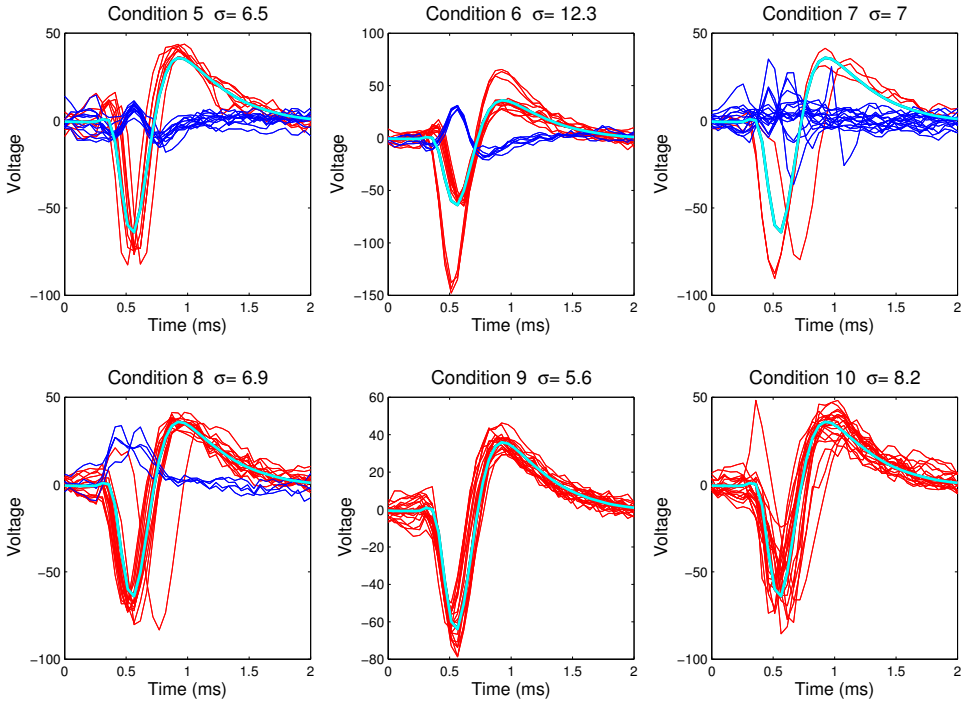

(b) Artifact substracted residuals

Figure 5: An example of failure in detection with axonal activation. Cyan trace: spike template, blue traces: trials with no spike, red traces: trials with spikes, black: artifact estimate